Enhancing Intraoperative Tissue Identification: Investigating a Smart Electrosurgical Knife's Functionality During Electrosurgery

Sara Azizian Amiri ⓘ, Jenny Dankelman ⓘ, and Benno H. W. Hendriks ⓘ

Abstract—*Objective:* **Detecting the cancerous growth margin and achieving a negative margin is one of the challenges that surgeons face during cancer procedures. A smart electrosurgical knife with integrated optical fibers has been designed previously to enable real-time use of diffuse reflectance spectroscopy for intraoperative margin assessment. In this paper, the thermal effect of the electrosurgical knife on tissue sensing is investigated.** *Methods:* **Porcine tissues and phantoms were used to investigate the performance of the smart electrosurgical knife after electrosurgery. The fat-to-water content ratio (F/W-ratio) served as the discriminative parameter for distinguishing tissues and tissue mimicking phantoms with varying fat content. The F/W-ratio of tissues and phantoms was measured with the smart electrosurgical knife before and after 14 minutes of electrosurgery. Additionally, a layered porcine tissue and phantom were sliced and measured from top to bottom with the smart electrosurgical knife.** *Results: Mapping the thermal activity of the electrosurgical knife's electrode during animal tissue electrosurgery revealed temperatures exceeding 400 °C.* **Electrosurgery for 14 minutes had no impact on the device's accurate detection of the F/W-ratio. The smart electrosurgical knife enables real-time tissue detection and predicts the fat content of the next layer from 4 mm ahead.** *Conclusion*: **The design of the smart electrosurgical knife outlined in this paper demonstrates its potential utility for tissue detection during electrosurgery.** *Significance:* **In the future, the smart electrosurgical knife could be a valuable intraoperative margin assessment tool, aiding surgeons in detecting tumor borders and achieving negative margins.**

Sara Azizian Amiri is with the Department of Biomechanical Engineering, Faculty of Mechanical, Maritime, and Materials Engineering, Delft University of Technology, 2628 Delft, The Netherlands (e-mail: s.azizianamiri@tudelft.nl).
Jenny Dankelman is with the Philips Research, IGT & US Devices and Systems Department, The Netherlands.
Benno H. W. Hendriks is with the Department of Biomechanical Engineering, Faculty of Mechanical, Maritime, and Materials Engineering, Delft University of Technology, The Netherlands, and also with the Philips Research, IGT & US Devices and Systems Department, The Netherlands.

Index Terms—**Smart electrosurgical knife, margin assessment, diffuse reflectance spectroscopy, real-time tissue detection, tissue optics.**

I. INTRODUCTION

THE increasing rate of patients undergoing cancer surgeries demands new technologies that can assist surgeons in pinpointing the border of the cancerous growth from the surrounding healthy or benign tissue to achieve complete tumor resection and negative margin [1].

Diffuse reflectance spectroscopy (DRS) has been studied vastly for its application in detecting the tissue type and discriminating healthy tissue from malignant tissue [2], [3], [4], [5], [6], [7], [8], [9], [10], [11], [12]. In DRS the amount of light that travels inside the tissue between the emitting and collecting fiber after multiple scattering and absorption events is sec2 measured [13].

From the diffused reflectance response of the tissue, optical characteristics of the tissue such as absorption and scattering profile or the concentration of the known chromophores of the tissue can be determined [14]. This potential has prompted scientists to further explore the application of the DRS in detecting abnormal tissue and discriminating it from the surrounding benign tissue [2], [3], [4], [5], [6], [7], [8], [9], [10], [11], [12]. For instance, de Boer et al. demonstrated that breast malignant tissue can be distinguished from benign tissue either by comparing the parameters related to the concentration of chromophores such as fat content or fat-water ratio (F/W-ratio) of the tissues or the different features on the specific wavelength ranges (400 nm-1600 nm) of the DRS spectrum of the tissues [5], [15], [16].

Being non-destructive, providing real-time results without requiring any extra contrast agent/dye or prior tissue/patient preparation [5] would be the advantage of the DRS over other existing margin assessment techniques. Although the effectiveness of the DRS in the detection of malignant tissue has been studied widely, the appropriate approach to incorporate DRS into the surgical workflow is still unclear.

Lately, efforts have been made to investigate the integration of the DRS into the electrosurgical knife as the main instrument that commonly being used by surgeons during tumor excision [17].

While an electrosurgical knife with intraoperative real-time tissue recognition power can become a "Holy Grail" for every

surgeon performing cancer surgery, embedding DRS in the electrosurgical knife raises many challenges.

Adank et al. showed that tissue carbonization upon electrosurgery can change its optical properties and DRS response [18]. However, they also indicated that as long as a larger fiber distance is being used, the depth that light can travel inside the tissue becomes larger than the depth of the affected tissue (cut or coagulated tissue) by the electrosurgical knife. Hence by using a larger fiber distance the effect of the electrosurgery on the accurate DRS read-out and tissue recognition can be minimized [18].

Tissue debris as a byproduct of electrosurgery could also have a huge impact on the optical tissue read-out. In a prior study, we, the authors of the present research, investigated the effect of the tissue debris attachment on the tip of the optical fibers which were mounted on the tip of a blade shape electrode of the electrosurgical knife [17]. After 30 seconds of electrosurgery with this DRS-integrated electrosurgical knife, a layer of contamination was formed on the tip of the optical fibers which mostly consisted of carbonized tissue. Moreover, it has been indicated that, to the extent that this contamination was a thin layer of debris, it would not adversely affect DRS measurement and tissue detection [17].

However, during the actual surgery, the electrosurgical knife would be used for several minutes which can cause a large amount of debris attachment and further disrupt the DRS measurements [18]. Furthermore, the effect of the heat produced during the electrosurgery on the optical fibers and DRS read-out, which can gravely disturb the application of the DRS-integrated electrosurgical knife, has not still researched.

While the Smart Electrosurgical Knife has been initially designed and developed previously [17], [18], [19], design modifications are imperative to enhance its robustness during electrosurgery. The goal is to minimize debris attachment and prevent optical fiber deterioration, issues stemming from the excessive heat generated during the procedure. To this end, this paper addresses the following aspects: first, an exploration of the maximum temperature attainable during electrosurgery; next, an investigation into various electrode designs for the Smart Electrosurgical Knife to identify a design that effectively reduces the impact of heat and debris attachment, byproducts of the electrosurgery, on tissue optical readout. Finally, the functionality of the ultimate design in tissue detection during electrosurgery is examined using ex vivo animal tissue, along with a study involving phantoms.

Research findings have demonstrated significant variations in fat content (Fat%) and the ratio between fat and water content between healthy and malignant human breast tissue, highlighting their potential as distinguishing factors between the two tissue types [15], [16]. Consequently, in this paper, these parameters are employed to evaluate the performance of the smart electrosurgical knife in detecting tissues with varying fat content and its potential to identify positive resection margins. Here, the main application we foresee in the future for the smart electrosurgical knife is for breast conserving surgery (lumpectomy) since the main discriminative parameter between the healthy tissue and tumor tissue in this cancer was vastly researched by the researchers. However, the application of the device can further be prospected in other types of surgery in which the discrimination of the tissues is possible with the DRS.

II. METHODS

The primary objective of this paper is to identify and evaluate the optimal design for the smart electrosurgical knife, ensuring its durability against the elevated heat and debris generated during electrosurgery. To achieve this goal, a comprehensive series of experiments was conducted, following the outlined timeline: Initially, the temperature reached by the blade during electrosurgery was examined to ascertain the extent of temperature involved in the process (Section II-A). Subsequently, diverse design iterations were developed with the intention of meeting the specified requirements (Section II-B). Experiment setups, as detailed in Section II-C, encompassing the DRS measurement console, ex vivo animal tissue, and tissue-mimicking phantoms were established and used to assess the functionality of the designs. Subsequently, investigations were conducted to assess the performance of the designs, pre-select the promising design, and further explore its potential (Section II-D). These various designs were subjected to testing on animal tissue (Section II-D-1). Building upon the insights gained from these initial experiments, the most effective design was selected for further investigation. This subsequent phase involved testing the chosen design in electrosurgery settings similar to those employed by surgeons during breast cancer procedures, first on animal tissue (Section II-D-2 and II-D-3) and subsequently on a phantom model (Section II-D-4). Lastly, the smart electrosurgical knife, equipped with the optimized design, was utilized to take measurements while applying electrosurgery to layered animal and phantom tissues (Section II-D-5). The investigation aimed to determine the device's ability to distinguish distinct tissue layers prior to reaching the tissue borders.

A. Characterization of Heat Development During Electrosurgery

To determine the range of the temperature of the heat that the optical fibers can be exposed to during the electrosurgery, a thermal imaging infrared camera (FLIR E54 24°, Teledyne FLIR LLC, United States) was used to measure the thermal signature of the blade of the electrosurgical knife during electrosurgery on porcine belly tissue. The electrosurgical knife with a blade-shaped electrode (WEIDE, Hangzhou Valued Medtech Co.,Ltd, China) was used to cut the tissue in different modes and settings. Porcine belly was purchased from the local butcher. The effect of the electrosurgery settings on the temperature of the blade was investigated using an electrosurgery unit (Force FX, Valleylab, Medtronic plc, USA) which allowed the electrosurgery in different modes of Cut-Pure, Cut-Blend, Coagulation-Spray, Coagulation-Fulguration. In each mode, the cutting was performed with different cutting powers of 40 W, 50 W, and 60 W.

The electrosurgical knife was used to cut the tissue in each mode/each setting in a continuous mode for 1 minute (1 minute of tissue electrosurgery without stops). The thermal imaging
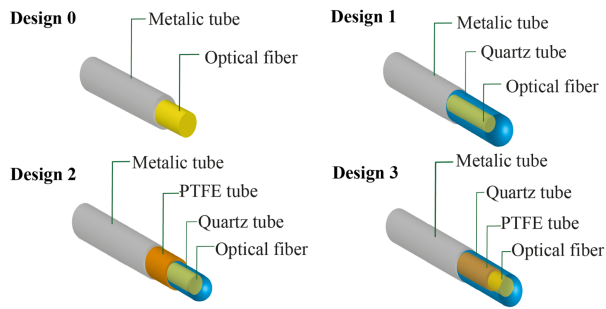
Fig. 1. Different mounting approaches for integrating optical fiber to the electrosurgical knife.

camera, which was fixed using the holders close to the electrosurgery setup, captured movies over the tissue while being cut/coagulated using the electrosurgical knife. Subsequently, the whole experiment was repeated, this time in an interrupted mode in which the knife was active (on) for 2 seconds and then inactive (off) for 2 seconds and this pattern was repeated till the whole electrosurgery time reached 2 minutes (in total 1 min active and 1 min inactive). The selection of these options was based on the results of research that investigated the most common electrosurgery settings and the time that surgeons spend in various surgeries [20]. The interrupted mode is more close to what happens in reality during surgery [20]. Then using the thermal imaging infrared camera and then software (FLIR ResearchIR MAX, Teledyne FLIR LLC, United States), the temperature of the tip of the blade (region of interest) in each pixel was recorded and the maximum temperature of it for each experiment was determined.

B. Heat and Debris Resistant Design of the Smart Electrosurgical Knife

Previously, the smart electrosurgical knife was developed by integrating DRS optical fibers into its structure. To date, two distinct designs have been documented. In the initial design (a prototype previously developed in [17], [18]), optical fibers were positioned within metallic tubes, which were affixed to the sides of a blade-shaped electrode using laser welding (Design 0). In the subsequent design iteration (Design 1), quartz tubes were added to the previous design to encapsulate the optical fibers on the blade-shaped electrode [19].

Given the adverse conditions of high temperature and debris exposure that the DRS optical fibers face during electrosurgery, this study introduces two additional distinct designs, referred to as Design 2 and Design 3, aimed at mitigating the adverse impact of heat on the optical fibers and DRS outputs. Depicted in Fig. 1 are these designs. Subsequently, the designs underwent testing to evaluate their efficacy and performance.

1) Description of Design 1: In Design 1 the optical fibers were first put inside quartz tubes (Hengshui Yuanbo Import And Export Co, China) with an inner diameter (ID) of 300 μm and an outer diameter (OD) of 1 mm.

2) Description of Design 2: In Design 2 heat shrinking Polytetrafluoroethylene (PTFE) tubes (Zeus Industrial Products,

Inc., United States) were first heated up while the quartz tubes (Hengshui Yuanbo Import And Export Co, China) with ID of 300 μm and OD of 500 μm was inside those to reach the right size then the optical fiber was placed inside the quartz tubes and the whole part were placed inside the metallic tubes.

3) Description of Design 3: In Design 3, first, the optical fibers were put inside the PTFE tubes (Zeus Industrial Products, Inc., United States) and then quartz tubes (Hengshui Yuanbo Import And Export Co, China) with ID 600 μm and OD 1 mm were used to surround the PTFE and optical fiber inside the metallic tubes.

C. Experimental Setup

To assess the smart electrosurgical designs and performance, the following experiment setups were used for further experimentation:

1) DRS Setup: The DRS setup comprises a measurement console, software for processing the measurements, and a custom-designed DRS needle probe.

Measurement console: For DRS measurements, a Philips custom-designed DRS console (Philips Research, Eindhoven) was used. The console includes a halogen broadband light source (Avantes, The Netherlands) and two spectrometers, one designated to collect the light in the 900–1700nm spectral range (NIRQuest 512, Ocean Optics, United States) and the other one in the 400-1000 nm spectral range (Maya2000 Pro, Ocean Optics, United States). One of the optical fibers was connected to the light source, the other one to the spectrometers, and the other end of the optical fibers was placed into the prototypes through different configurations. Before using each prototype, the optical console was calibrated thoroughly following the calibration process as mentioned in previous papers [3], [14], [21], [22]. Briefly, to calibrate the DRS console, the smart electrosurgical knife or the needle probe was placed at a fixed distance above a white reference standard (Spectralon with reflectivity of 99% for 400–1500 nm and >96% for 250–2000 nm, model: WS-1-SL, Labsphere Inc., United States) so that the distal end of the optical fibers become parallel to the surface of the standard. Subsequently, the spectral response of the white reference and a background measurement were recorded to minimize the influence of the ambient light [3], [14], [21], [22]. The calibration was performed once at the beginning of using each knife/probe.

Software: The DRS system outputs were processed using a Philips custom-developed software (Philips Research, Eindhoven). In this MatLab-based software a nonlinear Levenberg–Marquardt inversion algorithm based on an analytical model, first described by Farrell et al. [23], was used to fit a curve on the input spectrum which can be used further to calculate the concentration of the chromophore from the fitted data. More information about the method and model can be found in [3], [14]. Using the software each spectrum was analyzed and the fat fraction (Fat/Fat+water) and the total amount of fat and water content (Fat+Water) were extracted. More information regarding the DRS and its application in healthcare can be found in [4], [14], [22], [24].

TABLE I
MATERIAL AND THEIR CONCENTRATION USED IN PRODUCTION OF THE
PHANTOMS WITH DIFFERENT AMOUNT OF FAT AND WATER

	Role	Amount for 100 ml Phantom X%
Lard (ml)	To simulate the fat	X (ml)
Water (distilled) (ml)	To simulate the water	100-X (ml)
Gelatin (g)	Gelling agent and fat-water emulsifier	15% of water volume
Transglutaminase (g)	Cross linker of gelatin to increase the thermal stability	10% of Gelatin weight
Sodium Benzoate (g)	Preservative agent	0.1% of water volume

Custom-designed DRS needle probe: Furthermore, in experiments described in Section II-D-2, II-D-3, and II-D-4, a custom-designed DRS needle probe was also utilized, as employed in the author's previous research [17], [19], [21]. This probe featured a configuration that incorporated two optical fibers aligned in parallel with the probe's vertical axis, ensuring precise alignment of the fiber tips with the probe tip. With a functional fiber distance (FD) of 3.8 mm, this probe closely matched the FD of the smart electrosurgical knives.

Importantly, the design of the probe excluded the supplementary components found in the smart electrosurgical knife—components primarily designed to safeguard the optical fibers during electrosurgical procedures. Consequently, the outcomes obtained from these measurements serve as a control group, aimed at thoroughly investigating the impacts of integrating these supplementary components and the design of the smart electrosurgical knife on the measurement accuracy achieved by the prototypes.

2) Ex Vivo Animal Tissue Model: Fresh ex vivo porcine belly tissue (purchased from the local butcher), adipose and muscle tissue, were utilized consistently in the experiments, serving both as a substrate for electrosurgery and as a sample for diffuse reflectance spectroscopy (DRS) measurements. Furthermore, in specific experiments, chicken liver tissue was employed as an additional sample for electrosurgery to deliberately contaminate the electrosurgical knife. The liver tissue, abundant in blood content, was chosen to compensate for the absence of blood in the porcine tissue.

3) Tissue-Mimicking Phantoms to Assess Fat/Water Content: Tissue-mimicking phantom materials with tunable optical characteristics were developed to investigate the smart electrosurgical knives in a more controlled setup. These phantoms were produced with different and specific fat and water content to mimic tissues with various fat-to-water ratios. In comparison to animal tissue, these tissue-mimicking phantom materials have a more homogeneous composition, ensuring a reliable comparison between measurement results. The production process of these phantoms was previously described in [21]. Additionally, the materials utilized for producing the phantoms are detailed in Table I. Briefly, lard - pure porcine fat- (BEEF&STEAK (https://beefensteak.nl/), Netherlands), distilled water, gelatin (250 Bloom, ES1477, Natural Spices, Netherlands) as an emulsifier and gelling agent, Transglutaminase (TG) (unique products Schuurman, Netherlands) as cross-linker, and sodium benzoate

(a)																																			(b)

Fig. 2. Ex vivo animal tissues used in the experiments, with specific details provided in Section II-C. In the image (a), three sections of porcine adipose tissue (on the left) and muscle tissue (on the right) are presented. These tissue samples were employed for diffuse reflectance spectroscopy (DRS) measurements and were secured onto the plate using gray tapes. In image (b), the representation features the porcine tissue that underwent electrosurgery.

(SB) (Natural Spices, Netherlands) as preservation agent were used to produce the phantom.

First, depending on the required fat content of the phantom, the mixture of the water and SB was heated in a beaker on a heater stirrer till the temperature reached 50 °C. Then the gelatin powder was added slowly to the mixture and the whole liquid was then heated up. When the temperature of the mixture reached 90 °C, the lard was added to it and the beaker remained on a stirrer for a few more minutes and then the TG was added slowly to it. After 10 minutes the content of the beaker was poured on the molds and placed inside the freezer. After an hour the mold was removed from the freezer and the content of it was placed in the fridge overnight.

D. Performance Assessment

1) DRS Measurements to Preselect the Promising Design: To identify the most efficient design that can effectively protect the performance of the DRS during electrosurgery, the developed prototypes were tested in different experiments involving DRS measurements before and after electrosurgery on ex vivo animal tissue. To investigate the effect of electrosurgery on the DRS performance, one prototype from each design was produced and used to measure fixed locations on three pieces of fresh porcine adipose tissue and three pieces of fresh porcine muscle tissue (purchased from the local butcher), as depicted in Fig. 2(a). Then each prototype was used for electrosurgery on a large piece of porcine belly tissue, as depicted in Fig. 2(b) (mixes of fatty and muscle tissue) for 2 minutes in continuous mode (2 minutes active time) in the electrosurgery mode of Cut-Pure-60 W. Then the used prototype was used again to take DRS measurement from the same fixed location on adipose and muscle tissue. Then the process was repeated this time with cutting 1 minute (1 minute active time) and again the same fixed tissue locations were measured. The second step was repeated two more times to reach a total of 5 minutes of electrosurgery. With this process, it was possible to compare the DRS spectra of the same location measured with a prototype that was used for electrosurgery in different durations so that the effect of electrosurgery (heat and debris attachment) on tissue measurements could be studied.

By comparing the overall shape of the spectra and the calculated F/W-ratios between the fixed location measured with the unused prototype (before electrosurgery) and then the used prototype (after electrosurgery), it was possible to identify the most promising design. The results of these experiments unveiled the promising nature of the electrosurgical knife with Design 2. Subsequently, this design was selected for use in the subsequent experiments to further explore its application.

2) DRS Measurements in an Interrupted Electrosurgery: Design 2. which exhibited the most promising outcomes in the previous experiment was used for further investigations to determine its fullest potential. During a lumpectomy surgery, the electrosurgical knife usually is active on average for 2 seconds (0.6 s-3.8 s, measured for 23 lumpectomy surgery) [20] and in general, based on a surgical observation the whole activation time of the electrosurgical knife (sum of the time of each activation period) during the lumpectomy surgery is around 3.5 minutes to 7 minutes [25].

The smart electrosurgical knife with Design 2 (based on the outcomes of the previous experiment) was tested in a realistic setup similar to the lumpectomy surgery to indicate whether it can withstand the harsh environment during the lumpectomy electrosurgery and can accurately detect the tissue even after being used for several minutes. To resemble the previous experiment, pork muscle and fat tissue along with fresh chicken liver were used for the electrosurgery to contaminate the electrosurgical knife. The liver tissue with high blood content was used to compensate for the lack of blood in the porcine tissue.

Similar to the previous experiment, the chosen prototype was used for cutting the animal tissues for different durations in the interrupted (2 seconds on-2 seconds off) in Cut-Pure mode with the power of 60 W. Before using the prototype and then after every 2 minutes of cutting (in total 1 min activation time and 1 min inactivation time), DRS spectra were taken from a specific locations on 3 pieces of porcine muscle tissue and 3 pieces of porcine adipose tissue, similar to the figure shown in Fig. 2(a). This process was repeated seven times to reach the total cutting duration of 14 minutes (7 minutes on- 7 minutes off). Furthermore, the custom-designed DRS needle probe was also utilized, as employed in the author's previous research [17], [19], [21]. The probe was employed to conduct DRS measurements at fixed locations on sections of porcine tissue. Then the outputs of the DRS console were explored through the same method mentioned in the previous sections using the Philips custom-designed software. The performance of Design 2 was evaluated by comparing variations in the shape of spectra and the calculated F/W-ratios of measurements obtained using the smart electrosurgical knife used for different durations of electrosurgery, as well as those taken with the optical needle probe.

3) DRS Measurements in an Extended Electrosurgery: In previous experiments, the electrosurgical knife was deactivated for DRS measurements of porcine tissue after every 2 minutes of electrosurgery (1 minute active-1 minute inactive), whereas, during lumpectomy surgery, the electrosurgical knife can remain active for more extended periods [20], [25], subjecting the blade design to higher temperatures. To investigate the impact of prolonged electrosurgery on the smart electrosurgical

knife's performance, this experiment involves using the smart electrosurgical knife with the promising design to perform electrosurgery (Cut-Pure-40W) on porcine tissue and chicken liver tissue for a continuous 14-minute duration (with no intervening measurement sessions) in an interrupted mode (2 seconds on-2 seconds off), subsequent to the initial DRS measurements from porcine adipose and muscle tissue (3 separate pieces of each, at specific locations, similar to the figure shown in Fig. 2(a)). Afterward, DRS measurements from those specific porcine muscles and adipose pieces (same locations that were measured before electrosurgery) were carried out. This experiment was then performed again with a clean knife with Design 2 in the same condition only with a cutting power of 60W to compare the effect of the cutting power on the performance of the prototype and the final outcomes. The results of the DRS measurements then were interpreted using the same method mentioned in the last experiments. Furthermore, measurements taken by the needle probe from the specific location on the porcine muscle and adipose tissue were used as the control group, similar to the previous experiments. In a manner similar to the previous experiment, the spectral shape and calculated F/W-ratios were used to assess the performance of Design 2 in this experiment.

4) Fat and Water Content Estimation in Phantoms: One of the issues of using porcine tissue for comparing the DRS measurements (before and after surgery) is that whenever the tissue is pressed with the tip of the device, the tissue content moves slightly. Since the tissue composition is not homogeneous, with each small movement, the measured tissue can change a little, which could lead to small differences in the DRS response. Hence, the comparisons of the measurements taken with different probes from one specific location can be debatable. To address this issue, the homogeneous tissue-mimicking phantom with tunable fat and water content was produced (Section II-C-3) to investigate the performance of the prototype in a more controlled situation.

To determine if the smart electrosurgical knife with Design 2 can accurately estimate the fat content of the phantoms, tissue-mimicking phantom materials with Fat% of 0%, 5%, 15%, 20%, 40%, 50%, 60% were made following the process mentioned in the Section II-C-3. Moreover, a piece of lard (pure porcine fat) was used as a phantom material with Fat% close to 100%. Then from each phantom with different Fat%, DRS measurements were obtained from 3 different locations, once using a normal DRS needle probe (used as reference measurements as mentioned in previous sections) and once using a new smart electrosurgical knife. Then the Fat% and F/W-ratio of each spectrum were calculated and employed to assess the performance of Design 2.

For the second phantom study, the potential of the smart electrosurgical knife in accurate detection of the Fat% of the phantom after the knife was used for electrosurgery (used and contaminated) was tested. Similar to the experiment mentioned in previous sections, first a smart electrosurgical knife (Design 2) and then a needle probe (as reference) were used for measuring phantoms with Fat% of 10%, 40%, and 60%. Then the smart electrosurgical knife was used to cut porcine tissue (muscle and adipose) and chicken liver tissue for 14 minutes in an interrupted mode (2 seconds on- 2 seconds off) with electrosurgery settings

of Cut-Pure, once with the power of 40 W and once with the power of 60 W. Afterwards, measurements were acquired from the phantoms by the used/contaminated smart electrosurgical knife. Then the measured Fat% of each phantom taken by the needle probe, clean smart electrosurgical knife, and used smart electrosurgical knife were compared.

5) Real-Time Measurement During Cutting Layered Tissue and Phantom: A layered porcine tissue consisting of layers of adipose and muscle tissue, along with a layered phantom containing layers with different Fat% was prepared. The depth of the layers of the layered porcine tissue was not isometric or specified. However, each layer of the layered phantom had a 1 cm depth.

The smart electrosurgical knife was fixed on a vertical translation stage to set its height, while its horizontal movement was manually controlled. The tip of the knife was perpendicular to the top surface of the tissue/phantoms. The layered porcine tissue (placed on the back electrode of the electrosurgical unit) was cut (electrosurgery) from top to bottom with steps of 2 mm using the smart electrosurgical knife with the setting of Cut-Pure-60W (2 mm of cutting the tissue/phantom while the knife is active). After each 2 mm of cutting, the smart electrosurgical knife was stopped at the location, and DRS measurements were acquired. Then the process was repeated until the knife reached the bottom of the tissue/phantom. From the DRS spectra at each location, Fat% and F/W-ratio (as explained in the previous sections) were calculated and reported.

E. Statistical Analysis

On each measuring location on the porcine tissue or phantom material, three or four spectra were taken (different in each experiment). Moreover, the measurements were taken on three different locations (or pieces) which resulted in nine or twelve measurements in total for each tissue/phantom material in each experiment. The final spectrum of each measured location was averaged and shown in the graphs as the mean of these nine/twelve measurements $\pm$ SD (standard deviation, highlighted area). The measured Fat% or F/W-ratio was also reported as the mean $\pm$ SD of the calculated parameter from those nine/twelve measurements. Depending on the experiment the one-way or two-way ANOVA was used to statistically study the results and find evidence of any significant differences between the groups of the measurements. *p*-value less than 0.05 was considered significant (∗: p-value < 0.05, ∗∗:p-value < 0.01, ∗∗∗:p-value < 0.001). For the statistical analysis of the data or producing the graphs, MatLab (The MathWorks, Inc., Natick, Massachusetts, United States) and GraphPad Prism version 8.1.2 (GraphPad Software, La Jolla, CA USA, www.graphpad.com) were used.

III. RESULTS

A. Characterization of Heat Development During Electrosurgery

Fig. 3(a) shows the thermal image of the porcine tissue and the electrode during electrosurgery. The maximum temperate that
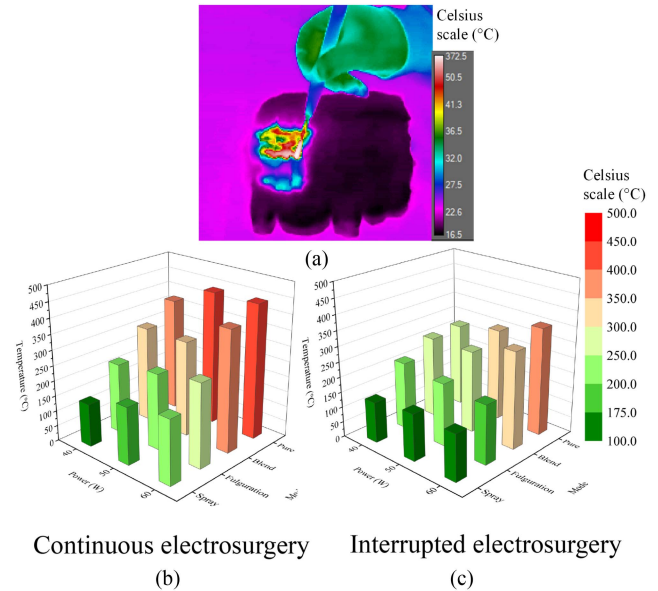

Fig. 3. Heat measurements during electrosurgery. (a) A typical image captured by the FLYR camera on the porcine tissue. (b) and (c) are showing the maximum temperature (°C) that the tip of the electrode of the electrosurgical knife reached during electrosurgery in different settings and powers. (b) Is showing the blade tip temperature in continuous electrosurgery and (c) is showing the blade tip temperature interrupted electrosurgery. The graphs were made with OriginPro 2015, OriginLab corporation, northampton, MA.

the tip of the electrode reached in continuous (1 minute) or interrupted (2 minutes, 2 seconds on- 2 seconds off) electrosurgery in different settings and powers are shown in Fig. 3(b) and (c). Electrosurgery in interrupted mode with cool-down periods corresponded with a lower temperature than electrosurgery in continuous mode. In both continuous and interrupted modes, in most cases, the maximum temperature of the blade increased by increasing the power from 40 W to 60 W. Electrosurgery in Cut-Pure produced the highest temperature in the blade (438.9 °C in continuous mode and 351.7 °C in interrupted mode) while the electrosurgery in coagulation modes (Fulguration and Spray) resulted in a lower temperature in the blades (≈ 100–200 °C).

B. Performance Assessment

1) DRS Measurements to Preselect the Promising Design: Design 0 was excluded from the experiments since after 1 minute of cutting the optical fibers were damaged and DRS measurement was not possible anymore.

Fig. 4. shows the results of DRS measurements, along with the calculated F/W-ratio, from fixed locations on three porcine muscle tissue samples and three porcine adipose tissue samples taken with the smart electrosurgical knives before electrosurgery and then after electrosurgery with the settings of Cut-Pure-60 W, in continuous mode and different durations (maximum 5 minutes). Since the measured F/W-ratio fluctuates largely for each design, the scale of the F/W-ratio diagram is adjusted differently for each design. In Design 1 the morphology of the DRS spectrum was changed noticeably after 2 minutes of electrosurgery. The most
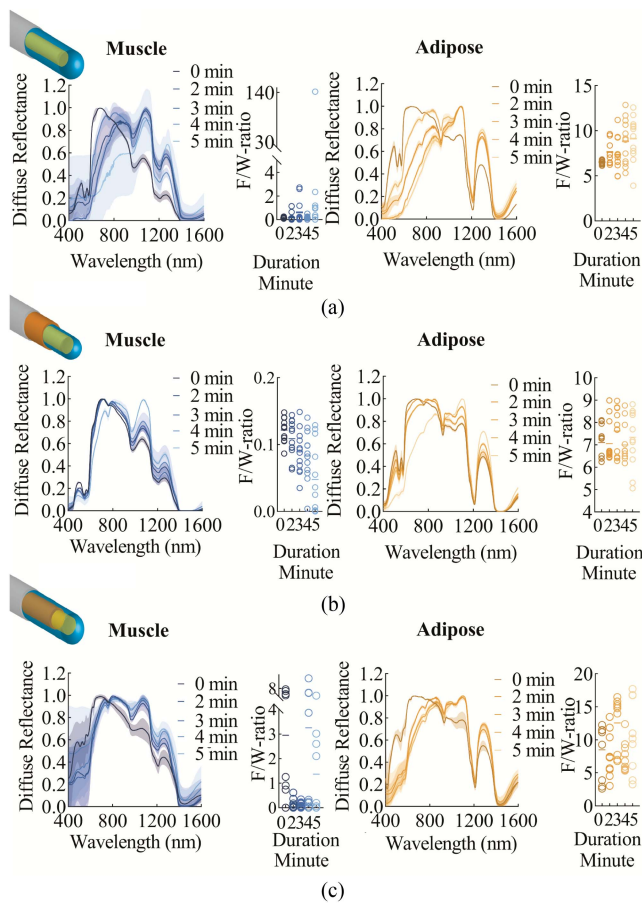
Fig. 4. Tissue detection results following continuous electrosurgery using different smart electrosurgical knife designs. Each design was employed to measure the diffuse reflectance spectroscopy (DRS) response of three pre-fixed adipose tissue samples and three pre-fixed muscle tissue samples (as depicted in Fig. 2(a)), both before (0 minutes) and after being subjected to electrosurgery at different durations. Electrosurgery was performed on separated pieces of the tissue shown in Fig. 1(b). Each measurement on each of these three tissue pieces was replicated four times, resulting in twelve measurements for each tissue type (muscle and adipose) at each duration of electrosurgery, ranging from 0 minutes to 5 minutes. The figure presents the averaged spectra of these 12 measurements with highlighted areas around the spectra indicating the standard deviation (SD). The data on the F/W-ratio scatterplot represent the calculated F/W-ratio from all twelve measurements on the specific tissue (three tissue pieces, with four replicates for each tissue piece, resulting in 12 measurements per tissue) after electrosurgery at different durations.

affected part of the spectrum is the Near-Infrared part which is the area where fat and water have the main absorption peaks (close to 1000 nm and 1200 nm). This explains the alternation of the F/W-ratio of the tissue, measured after using Design 1, especially for muscle tissue. Due to the low fat content of the muscle tissue, the F/W-ratio of this tissue is usually less than 1. On the contrary, the F/W-ratio of the muscle measured by the knife with Design 1 exceeds one when the knife is used for 2 minutes. Although the morphology of the adipose spectrum changes by increasing the duration of electrosurgery, the most affected part of the spectrum is in the visible wavelength ranges, which mostly corresponds to the blood content of the tissue. Hence, it is expected to see less fluctuation in the F/W-ratio of the

adipose tissue. In Design 3, not only does the shape of the spectra of both muscle and adipose tissue change after a few minutes of electrosurgery but also the F/W-ratio of both tissues changes significantly, making this design unreliable after electrosurgery. Contrastingly, when employing Design 2 for DRS measurement, the morphology of the spectrum for each tissue remains nearly unchanged even after 4 minutes of electrosurgery. However, the spectrum of the tissues changes significantly after 5 minutes of electrosurgery, especially in adipose tissue. The F/W-ratio of the tissues fluctuates less slightly in comparison to the other designs. Based on these outputs, this design (Design 2) was used for further investigations on settings more similar to realistic setups (Interrupted electrosurgery mode).

2) DRS Measurements in an Interrupted Electrosurgery Using Design 2: The results of the experiment in an interrupted electrosurgery mode are shown in Fig. 5. For each tissue type (muscle and adipose tissue) four measurements were done, each on three different locations, which results in twelve measurements per tissue. The spectra are shown as the average of these twelve spectra with the SD.

In Fig. 5(b) the results of DRS measurement in front of white reference (Spectralon) taken by needle probe and by a smart electrosurgical knife before electrosurgery and then after each time of electrosurgery are shown. The DRS spectrum for the needle probe and the unused and clean smart electrosurgical knife is the smooth line and similar to each other. Then after the electrosurgery the spectra change, mostly at visible light wavelengths (400–1000 nm). The dents on the spectra are at the wavelengths where absorption occurs in the blood (414 nm, 433 nm, 542 nm, 556 nm, 576 nm, 758 nm) and fat (760 nm, 930 nm, 1042 nm, 1211 nm, 1393 nm, and 1414 nm), showing that the source of these changes can be the tissue contamination (main contamination with blood and fat).

The overall shape of the spectra of the adipose and muscle tissue stayed almost the same when taken by the needle and the smart electrosurgical knife before and after electrosurgery (Fig. 5(c) and (e)). Some deviations were seen on the spectrum of the tissues measured by the needle probe and then the unused smart electrosurgical knife, mostly in the visible part (400 nm–800 nm) of muscle tissue and in the NIR part (800 nm–1600 nm) of adipose tissue. Subsequent to electrosurgery and then measurement using the smart electrosurgical knife, the spectrum of the muscle tissue was altered slightly in the NIR part while the spectrum of the adipose tissue was mostly changed in the visible light wavelengths.

However, the calculated F/W-ratio for each tissue taken by the smart electrosurgical knives after electrosurgery for different durations is not significantly different from the F/W-ratio measured using the needle probe or the clean (unused) smart electrosurgical knife. The results of the one-way ANOVA test on the multiple comparisons of the calculated F/W-ratio showed in most cases no significant differences between F/W-ratio of tissues measured by the needle probe, clean smart electrosurgical knife and then the smart electrosurgical knife after being used for electrosurgery in different durations.

The only significant difference was detected between the F/W-ratio of the adipose tissue measured with a smart electrosurgical
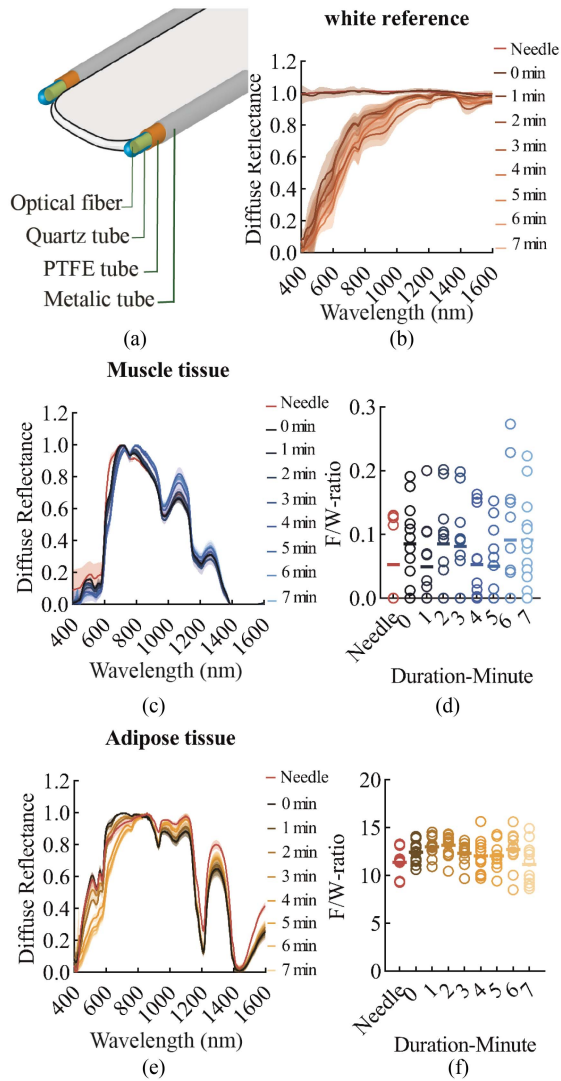
Fig. 5. Tissue detection results after interrupted electrosurgery using design 2. Durations of electrosurgery mentioned in minutes are the total activation time during 2 minutes of interrupted electrosurgery (2 seconds on-2 seconds off). Hence, 7 minutes duration means 14 minutes of interrupted electrosurgery. (a) Sketch of the design 2. (b) Spectrum of the needle probe and then the smart electrosurgical knife in front of the white reference before and after each 2 minutes of interrupted electrosurgery. After each 2 minutes of electrosurgery, the smart electrosurgical knife was used to measure the DRS response of (c) the muscle and (c) adipose tissue, and to calculate the F/W-ratio for (d) muscle and (f) for adipose tissue.
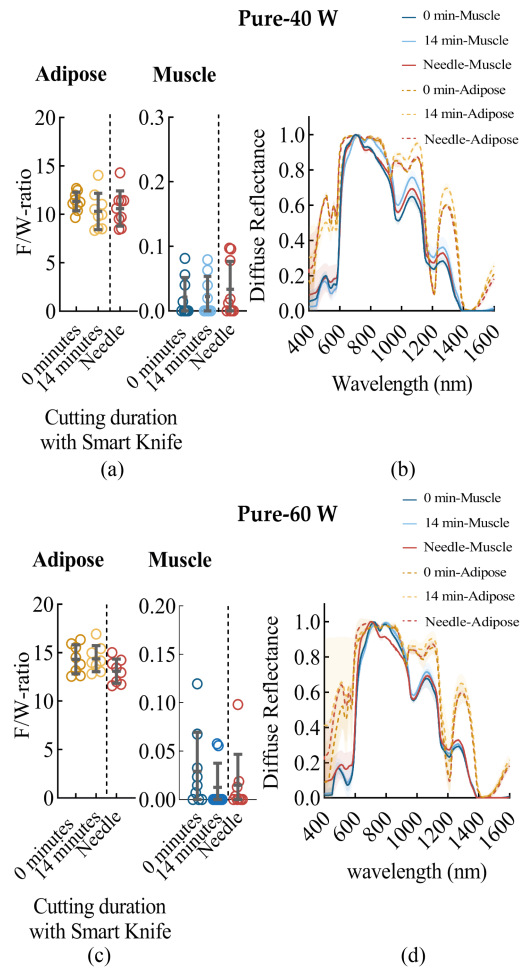

Fig. 6. Results of the smart electrosurgical knife (Design 2) after 14 minutes of electrosurgery in interrupted mode (2 seconds on-2 seconds off). (a) and (c) The measured F/W-ratio after the electrosurgery with power of 40 W (a) and 60 W (c) are shown for each tissue. (b) and (d) The average of the measured spectra of each tissue using the DRS needle probe, and the smart electrosurgical knife before and after the electrosurgery with power of 40 W (b) and 60 W (d).

knife after 2 minutes (4 minutes interrupted) and 7 minutes (14 minutes interrupted) electrosurgery with p = 0.035. Considering the non-significant deviation of the measured F/W-ratio by the smart electrosurgical knife after electrosurgery for extended durations, the muscle tissue (F/W-ratio < 0.3) and adipose tissue (F/W-ratio > 5) are easily detectable from each other.

3) DRS Measurements in an Extended Electrosurgery Using Design 2: The statistical analysis of the results (shown in Fig. 6(a) and (c)) showed no significant differences between the F/W-ratio measured before and after the electrosurgery with the smart electrosurgical knife and the needle shape DRS probe in both experiments. In Fig. 6(b) the average of the measured

spectrum using a needle probe, and the smart electrosurgical knife before and after electrosurgery for each tissue were displayed. Although there are some deviations between the measured spectra, these alterations had no significant effect on the measured F/W-ration of the tissues. After the electrosurgery with 60 W the average spectra of the tissues (shown in Fig. 6(d)), mainly the adipose tissue, showed more fluctuation, with larger SD, mostly at the visible wavelengths. In summary, electrosurgery did not have a negative impact on the results, demonstrating that even after 14 minutes of interrupted electrosurgery, the smart electrosurgical knife can still correctly measure the spectral response and F/W-ratio of the tissue.

4) Fat and Water Content Estimation in Phantoms Using Design 2: The results of DRS measurements on phantoms are shown in Fig. 7(a). Two-Way ANOVA was used for static analysis of the data. The results of the tests showed only a significant difference between the F/F+W of the Phantom 60% measured with a needle probe and the knife with p-<0.0001.
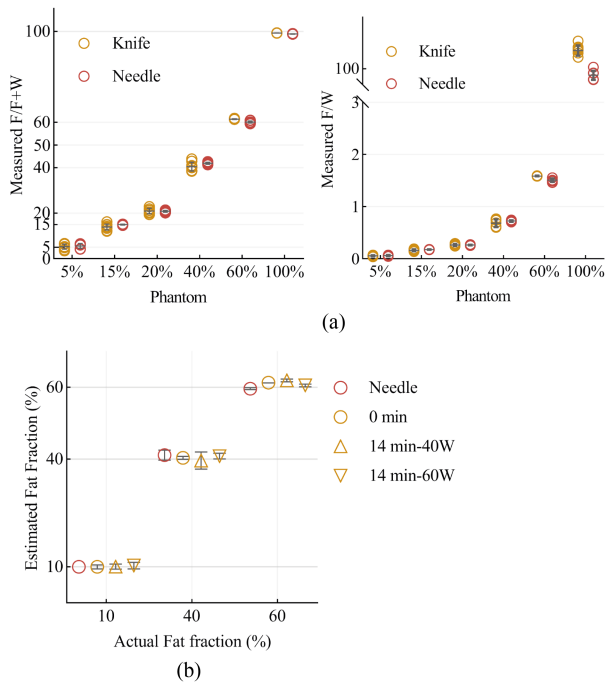
(a)

(b)

Fig. 7. Phantom measurements with the DRS optical needle and the clean and unused smart electrosurgical knife used on the different Phantoms X% (Table I). (a) Fat fraction, F/F+W, (b) F/W-ratio, and (c) F/F+W of the phantoms measured using needle probe, and the smart electrosurgical knife before and after using the knives for electrosurgery on animal tissue with different powers.

Fig. 8. Tissue detection results of the smart electrosurgical knife while cutting a layered tissue or phantom. (a) The layered tissue with layers of the adipose and muscle tissue. (b) Measured F/F+W and F/W-ratio of the layered tissue from top to bottom after each 2 mm of electrosurgery in this direction. (c) Layered phantom consisting of layers with different amount of fat. The number on the layers indicates the F/F+W of each layer. (d) Measured F/F+W and F/W-ratio of the layered phantom from top to bottom after each 2 mm of electrosurgery in this direction.

The mean F/F+W of the Phantom 60% measured with needle probe was 60.1% and with the knife was 61.38%. Moreover, significant differences between the F/W-ratio of the Phantom 60% measured using the probe (1.506) and the knife (1.587) were seen with a p-value of <0.0001. Furthermore, the test results showed a significant difference between the measured F/F+W and F/W-ratio of Phantom 100% using the probe (mean F/F+W of 98.86%, mean F/W-ratio of 87.3) and the knife (mean F/F+W of 99.26%, mean F/W-ratio of 135.5). There were no other statistical differences between other measurements and the calculated parameters related to the fat content of the phantoms measured using a smart electrosurgical knife or needle probe.

Fig. 7(b) shows the F/F+W of the phantoms measured using a needle probe, an unused smart electrosurgical knife, and then the smart electrosurgical knives used for electrosurgery with different powers. The results of statistical analysis on the F/F+W showed no significant differences between the fat content of the phantoms measured before and after the electrosurgery using the smart electrosurgical knife.

5) Real-Time Measurement During Cutting Layered Tissue and Phantom: Layered porcine tissue (Fig. 8(a)) and phantom (Fig. 8(c)) were cut and measured using a smart electrosurgical knife from top to bottom. The graph in Fig. 8(b) presents the measured F/F+W and F/W-ratio of the locations with a 2 mm distance from each other on the layered tissue, which shows a clear transition between the layers. Since there was no control over the tissue in front of the knife, the experiment was also
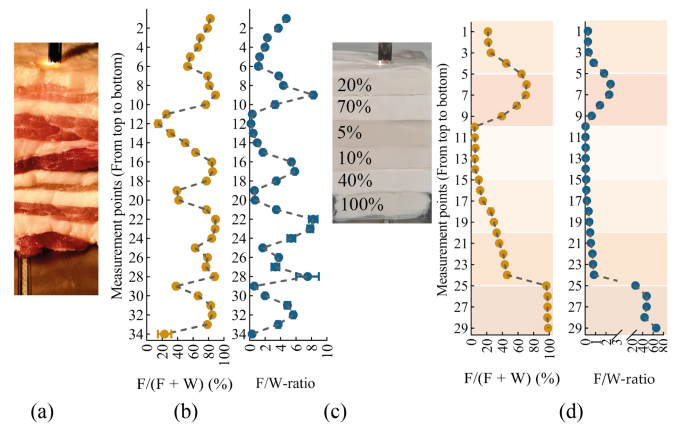
redone on a layered phantom in which each phantom had a specific depth and known concentration of fat and water.

The numbers on the layers in Fig. 8(c) show the F/F+W of that layer. The measured F/F+W and F/W-ratio of the phantom at each point (steps of 2 mm) are shown in Fig. 8(d). In this graph, the transition between layers is clearly visible. Interestingly, when transitioning from the top of one layer to the top of the next layer, both parameters, F/F+W and F/W-ratio, first reach the F/F+W and F/W-ratio of the layer that the blade is currently inside, and then, as the transition progresses, the parameter either decreases or increases based on the fat content of the next layer before reaching that layer. This shows that the smart electrosurgical knife can detect the layers of the phantom from a few millimeters before reaching the layer.

IV. DISCUSSION

In the pursuit of advancing the field, our study introduces substantial design modifications to elevate the capabilities of a smart electrosurgical knife. In this study, our primary goal was to address challenges related to heat-induced optical changes and debris attachment. Through the implementation of design enhancements, particularly the incorporation of quartz and PTFE tubes, we achieved promising results. This refined design was subsequently employed in a realistic setup, demonstrating its efficacy in providing reliable DRS measurements on porcine tissue and tissue-mimicking phantoms, even during prolonged electrosurgery sessions lasting up to fourteen minutes. Notably, the smart electrosurgical knife's improved design facilitated real-time measurements in the dynamic context of electrosurgery on layered porcine tissue and a layered phantom.

Difficulty in the detection of a safe tumor margin during cancer surgeries, such as breast lumpectomy, is an obstacle for surgeons which can result in a positive margin. In our previous research, we developed a smart electrosurgical knife with the

goal of providing surgeons with real-time tissue feedback to guarantee a negative margin as a result of cancer surgery [17], [18]. The initial iteration of the smart electrosurgical knife was made by integrating a normal electrosurgical knife with diffuse reflectance spectroscopy technology [17], [18]. In the current research, we aimed to further enhance the design of the smart electrosurgical knife and investigate its functionality during electrosurgery.

It has been shown that using DRS the composition of the tissue can be determined and therefore different tissues can be distinguished from each other. The application of the DRS in the detection of the tumor tissue from surrounding benign tissue for a variety of cancers has been studied in many research through the last decade, e.g., for breast cancer [3], [15], lung cancer [6], liver cancer [2], [10], skin cancer [11], cervical cancer [9], colorectal cancer [7] and oral cancer [8].

To measure the tissue using the DRS system, the optical fibers of the DRS setup (which are connected to a light source and the spectrometers) are required to be in close contact with the tissue. To do so, in the development of the smart electrosurgical knife, the optical fibers should be placed on the tip of the electrode of the knife such that they are positioned as much as possible close to the tissue during the electrosurgery. One of the main issues with this idea is the high temperature that the optical fibers can be exposed to during the electrosurgery which could destroy the fibers [17]. The other side effect of the heat is the tissue carbonization and debris attachment upon the electrosurgery which could affect the DRS measurements and tissue read-out [18].

Screening the thermal behavior of the electrode of the knife during the electrosurgery showed that the maximum temperature during electrosurgery in Pure-60W mode would be ≈438 °C, while usually in a breast cancer surgery the temperature (in a normal setting, 40 W) the maximum temperature would be between 200–300 °C.

One of the limitations of the heat measurement experiment was the attachment of debris (burned or unburned tissue) to the electrode of the electrosurgical knife during the electrosurgery. This phenomenon, along with the subsequent alterations in thermal emissivity dynamics, presents a significant consideration in the context of temperature measurement during electrosurgical procedures. In the future, it's important to improve the methodology of measuring temperatures during electrosurgery. This will involve using more controlled methods to better account for debris attachment and emissivity changes. These improvements are essential to ensure accurate temperature measurements.

Besides the exposure to the high temperature, the debris attachment [17] and mechanical damages (while using the knife and also during cleaning cycles) could affect the optical fibers that were placed close to the tip of the electrode of the electrosurgical knife. Therefore, the encapsulation of the optical fiber inside quartz was used as an approach to protect those from destructive conditions. Among the different investigated designs in this research, Design 2, in which an extra PTFE tube was used around the quartz tubes, showed the most promising results. In Designs 1 and 3, considerable spectra and F/W-ratio alterations were seen after only one minute of electrosurgery, indicating

that the optical fibers could be damaged and that the housings could not protect the fibers completely. Besides, in Design 3, the variation of the average spectrum in each electrosurgery duration was large which could be due to the PTFE tube around the optical fiber. It is noteworthy to emphasize that throughout all experiments, a clear distinction was maintained between the tissues utilized for the electrosurgery procedures and those designated for measurements. Measurements were consistently performed at predefined, fixed locations on separate tissue pieces, which remained intact throughout each experiment's duration. This approach established a constant reference point for measurements, ensuring that any observed variations primarily stemmed from differences in the electrosurgical knife design rather than potential changes in the tissue itself.

During the continuous electrosurgery in Pure-60W mode, the smart electrosurgical knife with Design 2 could still measure the tissue accurately. After 4 or 5 minutes of electrosurgery in this mode, some changes in the overall shape of the spectra of the tissue were noticeable, mostly in the visible wavelengths. However, continuous electrosurgery in 60 W and pure mode is an uncommon setting for cancer surgery. During a normal lumpectomy surgery, the common electrosurgery setting is 35-40 W in the blend or pure cutting mode [20] which can result in lower temperatures and a less distractive environment. Moreover, the measurement of the electrosurgical unit activation time during lumpectomy surgery showed that each time activation of the knife lasts on average for 2 seconds (0.6-3.8 s) [20]. Accordingly, in the next experiments, the smart electrosurgical knife with Design 2 was used in a more realistic setting and in interrupted electrosurgery mode with cycles of 2 seconds on - 2 seconds off. The spectrum taken by the smart electrosurgical knife in front of the white reference after the electrosurgery was not the same as the spectra of the knife before surgery and the needle probe. These alterations in the spectra were due to the tissue contamination mostly with blood and fat. These results are in line with what is reported in [17], in which the same alternation on the spectrum was seen and chemical analysis of the contamination on the tip of the optical fibers showed that the contamination is mostly carbonized tissue along with traces of biological components such as Na and Mg [17].

Although the contamination was seen in front of the optical fiber (on the outer side quartz tube) which also altered slightly the spectra of the adipose and muscle tissue in some wavelengths, these contaminations could not affect the measured F/W-ratio of the tissue significantly in comparison to the F/W-ratio measured with the clean/unused smart electrosurgical knife before electrosurgery. The same results were also achieved when the smart electrosurgical knife was used for 14 minutes of electrosurgery in interrupted mode (2 seconds on - 2 seconds off) with different powers (40 W and 60 W). Despite some variations that occurred in the spectrum of each tissue measured after electrosurgery, the measured F/W-ratio did not fluctuate largely. Indicating that even after 14 minutes of electrosurgery with a power of 60 W in an interrupted setting, the type of the tissue is detectable, and tissues can be distinguished from each other. There were some statistically non-significant but noticeable deviations between the F/W-ratio of the tissues measured using the smart electrosurgical

knife and needle probe. The source of these variations could be due to the different optical fibers that have been used to produce the probes or the small difference between the fiber distance of the needle probe (3.8 mm) and the smart electrosurgical knife (3.87 mm).

A tissue-mimicking phantom with known composition was used in this research to investigate the tissue detection power of the smart electrosurgical knife in a more controlled approach. The phantoms were created using the formulation originally introduced in our previous study [21]. In this paper, we showed that a phantom with different fat content can be produced to closely represent the DRS profile of real human breast tissue as well as porcine tissue [21]. Similarly, in this research phantoms with a fat content from 5% to 100% were produced. The DRS measurement using the DRS needle probe and then the unused smart electrosurgical knife from these phantoms showed that using both devices results in the same measurements. Although a statistically significant difference was seen between the F/F+W of the Phantom 60% measured with needle probe and the measured with the smart electrosurgical knife, the difference was too small (60.10% and 61/38%) that would not affect the tissue discrimination. Usually, tissue classification is more difficult in the border area or location with mixed tissues that contain both connective and malignant tissue. In those areas, the fat content of the tissues is more similar which complicates the tumor margin detection [5]. The extent to which these small variations, such as the one detected between the F/F+W of the Phantom 60% or other disparities between the F/W-ratio measured with a needle probe and the smart electrosurgical knife, could affect human breast tissue classification is a subject that may be explored in future studies using an ex vivo lumpectomy sample experiment.

The considerable difference between the F/W-ratio of the Phantom 100% measured with a smart electrosurgical knife and the probe are due to the fact that in higher fat percentages small deviations in F/F+W results in large deviations in F/W-ratios. However, in reality, the effect of this variation on tissue detection could be insignificant, since the difference between the fat content and the F/W-ratio of the breast malignant tissue and adipose tissue is very large [16].

The results of DRS measurement using the smart electrosurgical knife from the phantoms (Phantom 10%, Phantom 40%, and Phantom 60%) before and after electrosurgery indicated that even 14 minutes of electrosurgery with the high powers of 40 W and 60 W did not affect the accuracy of the prototype in detecting the F/W-ratio of the phantoms. These results showed that the encapsulation of the optical fibers in Design 2 can protect the fibers for at least 14 minutes of electrosurgery. While the results were statistically stable, and the differences in the numbers were negligible in this research, more investigation is required in the future on human tissue samples to analyze the magnitude of the effect of these small variations on the tissue discrimination power of the smart electrosurgical knife.

The experiment on the layered tissue and layered phantom showed the potential of the smart electrosurgical in detecting each layer based on its fat and water content. Besides, more remarkably, the results of these experiments revealed that the smart electrosurgical knife can predict the presence of the next

layer before reaching it. Based on the F/F+W and F/W-ratio graph shown in Fig. 8, it is perceptible that from 4 mm before the tip of the knife reaches the next layer, the measured fat content of the tissue increases or decreases depending on the fat content of the next layer. Based on the literature, the penetration depth of the light in the DRS probe increases by increasing the fiber distance [26], [27]. The results of the experiment on layered phantom showed that the smart electrosurgical knife renders detecting the changes in layers of the phantom from 4 mm ahead. Determining the maximum margin that the smart electrosurgical knife with the current design can detect before reaching the next layer can be an interesting topic for future research. During cancer surgery, the surgeon aims to achieve more than 2 mm of margin around the tumor to decrease the rate of positive margin and the recurrence rate [28], [29]. In 2019 Baltussen et al. investigated the effect of the tumor distance from the top surface on the accuracy of the tissue classification and showed that when an FD of 2 mm is used, the accuracy decreases when the distance of the tumor from the surface goes beyond 1.5 mm [30]. Hence, in this research, the large fiber distance of the smart electrosurgical knife has become beneficial in the scene that can accomplish the 4 mm detection depth. However, while all these assumptions are practical in a homogenous tissue or phantom, in reality, surgeons mostly face complex and heterogynous compositions of tissue in which the usability of the smart electrosurgical knife has not been tested yet. In future, the smart electrosurgical knife accuracy and detection depth need to be investigated on more complex tissue composition, either on ex vivo or in vivo breast tissue in locations where multiple tissues are present or on heterogeneous phantoms. Ultimately, in the next steps, tissue classification methods and algorithms can be developed to find the correlation between the changes in the F/W-ratio or the specific features on the spectrum to the type of specific tissue and the distance of the tip of the knife from it.

V. CONCLUSION

Our investigation revealed that, under various electrosurgery settings, the generated heat can reach temperatures exceeding 400 degrees. This study aimed to mitigate the associated challenges, particularly heat-induced optical changes and debris attachment, through the implementation of design enhancements in the smart electrosurgical knife. Design 2, distinguished by its incorporation of quartz and PTFE tubes, emerged as the most promising iteration and underwent further examination under realistic setups, including interrupted electrosurgery modes. The results underscored the remarkable resilience of Design 2, demonstrating its ability to provide reliable diffuse reflectance spectroscopy (DRS) measurements on porcine tissue and tissue-mimicking phantoms, even after prolonged electrosurgery sessions lasting up to fourteen minutes. Furthermore, the smart electrosurgical knife's design facilitated real-time measurements during electrosurgery on layered porcine tissue and a layered phantom. This capability, evident in detecting transitions between tissue/phantom layers with varying fat and water content and predicting the fat content of the next layer

from a distance of 4 mm ahead, holds significant promise for precise intraoperative margin assessment.

Our findings not only confirm the resilience and reliability of the smart electrosurgical knife in challenging surgical conditions but also underscore its potential significance for future applications. Particularly in surgeries where precise tissue discrimination is essential, the successful real-time measurements during electrosurgery and the predictive capabilities for tissue characteristics highlight the device's promising role in enhancing surgical precision and ultimately contributing to optimal clinical outcomes.

ACKNOWLEDGMENT

REFERENCES

[1] J. Heidkamp et al., "Novel imaging techniques for intraoperative margin assessment in surgical oncology: A systematic review," *Int. J. Cancer*, vol. 149, no. 3, pp. 635–645, 2021.

[2] J. W. Spliethoff et al., "In vivo characterization of colorectal metastases in human liver using diffuse reflectance spectroscopy: Toward guidance in oncological procedures," *J. Biomed. Opt.*, vol. 21, no. 9, 2016, Art. no. 097004.

[3] R. Nachabé et al., "Diagnosis of breast cancer using diffuse optical spectroscopy from 500 to 1600 nm: Comparison of classification methods," *J. Biomed. Opt.*, vol. 16, no. 8, 2011, Art. no. 087010.

[4] R. Nachabé et al., "Effect of bile absorption coefficients on the estimation of liver tissue optical properties and related implications in discriminating healthy and tumorous samples," *Biomed. Opt. Exp.*, vol. 2, no. 3, pp. 600–614, 2011.

[5] L. L. de Boer, "Detecting breast cancer tissue with diffuse reflectance spectroscopy," Ph.D. dissertation, Univ. Twente, 2019.

[6] J. W. Spliethoff et al., "Spectral sensing for tissue diagnosis during lung biopsy procedures: The importance of an adequate internal reference and real-time feedback," *Lung Cancer*, vol. 98, pp. 62–68, 2016.

[7] M. S. Nogueira et al., "Evaluation of wavelength ranges and tissue depth probed by diffuse reflectance spectroscopy for colorectal cancer detection," *Sci. Rep.*, vol. 11, no. 1, pp. 1–17, 2021.

[8] G. Einstein et al., "Diffuse reflectance spectroscopy for monitoring physiological and morphological changes in oral cancer," *Optik*, vol. 127, no. 3, pp. 1479–1485, 2016.

[9] V. G. Prabitha et al., "Detection of cervical lesions by multivariate analysis of diffuse reflectance spectra: A clinical study," *Lasers Med. Sci.*, vol. 31, no. 1, pp. 67–75, 2016.

[10] A. Keller et al., "Diffuse reflectance spectroscopy of human liver tumor specimens-towards a tissue differentiating optical biopsy needle using light emitting diodes," *Biomed. Opt. Exp.*, vol. 9, no. 3, pp. 1069–1081, 2018.

[11] Y. Zhang et al., "Diffuse reflectance spectroscopy as a potential method for nonmelanoma skin cancer margin assessment," *Transl. Biophotonics*, vol. 2, no. 3, 2020, Art. no. e202000001.

[12] A. Garcia-Uribe et al., "In vivo diagnosis of melanoma and nonmelanoma skin cancer using oblique incidence diffuse reflectance spectrometry," *Cancer Res.*, vol. 72, no. 11, pp. 2738–2745, 2012.

[13] R. Nachabé, "Diagnosis with near infrared spectroscopy during minimally invasive procedures," Ph.D. dissertation, Radiotherapy, Erasmus MC, Rotterdam, 2012.

[14] R. Nachabé et al., "Estimation of biological chromophores using diffuse optical spectroscopy: Benefit of extending the UV-VIS wavelength range to include 1000 to 1600 nm," *Biomed. Opt. Exp.*, vol. 1, no. 5, pp. 1432–1442, 2010.

[15] L. L. De Boer et al., "Towards the use of diffuse reflectance spectroscopy for real-time in vivo detection of breast cancer during surgery," *J. Transl. Med.*, vol. 16, no. 1, pp. 1–14, 2018.

[16] L. L. De Boer et al., "Fat/water ratios measured with diffuse reflectance spectroscopy to detect breast tumor boundaries," *Breast Cancer Res. Treat.*, vol. 152, no. 3, pp. 509–518, 2015.

[17] S. A. Amiri et al., "Intraoperative tumor margin assessment using diffuse reflectance spectroscopy: The effect of electrosurgery on tissue discrimination using ex vivo animal tissue models," *Biomed. Opt. Exp.*, vol. 11, no. 5, pp. 2402–2415, 2020.

[18] M. W. Adank et al., "Real-time oncological guidance using diffuse reflectance spectroscopy in electrosurgery: The effect of coagulation on tissue discrimination," *J. Biomed. Opt.*, vol. 23, no. 11, 2018, Art. no. 115004.

[19] S. A. Amiri et al., "Electrosurgical knife equipped with diffused reflectance spectroscopy sensing for tumor margin detection during breast conserving surgery: A phantom study," *Proc. SPIE*, vol. 11631, pp. 49–57, 2021.

[20] F. C. Meeuwsen, "Safe surgical signatures," Ph.D. dissertation, Mech., Maritime Mater. Eng., Delft Univ. Technol., 2019.

[21] S. A. Amiri et al., "Tissue-mimicking phantom materials with tunable optical properties suitable for assessment of diffuse reflectance spectroscopy during electrosurgery," *Biomed. Opt. Exp.*, vol. 13, no. 5, pp. 2616–2643, 2022.

[22] R. Nachabe et al., "Estimation of lipid and water concentrations in scattering media with diffuse optical spectroscopy from 900 to 1600 nm," *J. Biomed. Opt.*, vol. 15, no. 3, 2010, Art. no. 037015.

[23] T. J. Farrell et al., "A diffusion theory model of spatially resolved, steady-state diffuse reflectance for the noninvasive determination of tissue optical properties in vivo," *Med. Phys.*, vol. 19, no. 4, pp. 879–888, 1992.

[24] T. M. Bydlon et al., "Chromophore based analyses of steady-state diffuse reflectance spectroscopy: Current status and perspectives for clinical adoption," *J. Biophotonics*, vol. 8, no. 1/2, pp. 9–24, 2015.

[25] F. Mollerus, "The integration of diffuse reflectance spectroscopy into the electrosurgical knife used during breast-conserving surgery," M.S. thesis, Mech., Maritime Mater. Eng., Delft Univ. Technol., 2018.

[26] H. Arimoto et al., "Depth profile of diffuse reflectance near-infrared spectroscopy for measurement of water content in skin," *Skin Res. Technol.*, vol. 11, no. 1, pp. 27–35, 2005.

[27] R. Hennessy et al., "Effect of probe geometry and optical properties on the sampling depth for diffuse reflectance spectroscopy," *J. Biomed. Opt.*, vol. 19, no. 10, 2014, Art. no. 107002.

[28] C. Kunos et al., "Breast conservation surgery achieving ≥ 2 mm tumor-free margins results in decreased local-regional recurrence rates," *Breast J.*, vol. 12, no. 1, pp. 28–36, 2006.

[29] N. Houssami et al., "The association of surgical margins and local recurrence in women with early-stage invasive breast cancer treated with breast-conserving therapy: A meta-analysis," *Ann. Surg. Oncol.*, vol. 21, no. 3, pp. 717–730, 2014.

[30] E. Baltussen et al., "Tissue diagnosis during colorectal cancer surgery using optical sensing: An in vivo study," *J. Transl. Med.*, vol. 17, no. 1, pp. 1–10, 2019.